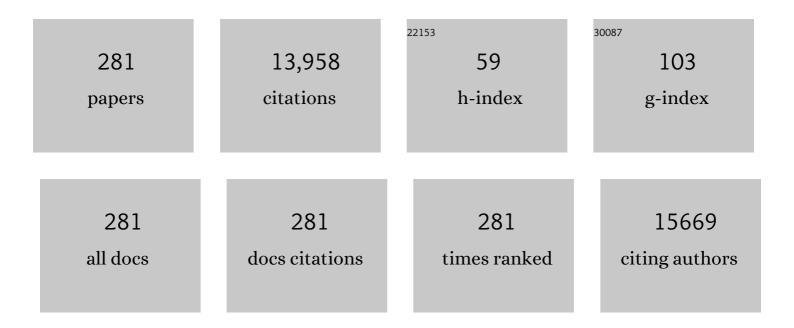
List of Publications by Year in descending order

Source: https://exaly.com/author-pdf/8368885/publications.pdf Version: 2024-02-01



SHUUNLIAO

#	Article	IF	CITATIONS
1	High Performance Fe- and N- Doped Carbon Catalyst with Graphene Structure for Oxygen Reduction. Scientific Reports, 2013, 3, .	3.3	514
2	An Isolated Zinc–Cobalt Atomic Pair for Highly Active and Durable Oxygen Reduction. Angewandte Chemie - International Edition, 2019, 58, 2622-2626.	13.8	494
3	Current research trends and perspectives on materials-based hydrogen storage solutions: A critical review. International Journal of Hydrogen Energy, 2017, 42, 289-311.	7.1	440
4	Effect of Transition Metals on the Structure and Performance of the Doped Carbon Catalysts Derived From Polyaniline and Melamine for ORR Application. ACS Catalysis, 2014, 4, 3797-3805.	11.2	351
5	Transition Metal Nitride Coated with Atomic Layers of Pt as a Low-Cost, Highly Stable Electrocatalyst for the Oxygen Reduction Reaction. Journal of the American Chemical Society, 2016, 138, 1575-1583.	13.7	348
6	Base-Free Oxidation of Alcohols to Esters at Room Temperature and Atmospheric Conditions using Nanoscale Co-Based Catalysts. ACS Catalysis, 2015, 5, 1850-1856.	11.2	291
7	High Performance PtRulr Catalysts Supported on Carbon Nanotubes for the Anodic Oxidation of Methanol. Journal of the American Chemical Society, 2006, 128, 3504-3505.	13.7	280
8	Controlled-Access Hollow Mechanized Silica Nanocontainers. Journal of the American Chemical Society, 2009, 131, 15136-15142.	13.7	272
9	Selective Oxidation of Saturated Hydrocarbons Using Au–Pd Alloy Nanoparticles Supported on Metal–Organic Frameworks. ACS Catalysis, 2013, 3, 647-654.	11.2	211
10	Structural defects in metal–organic frameworks (MOFs): Formation, detection and control towards practices of interests. Coordination Chemistry Reviews, 2017, 349, 169-197.	18.8	200
11	Well-Defined ZIF-Derived Fe–N Codoped Carbon Nanoframes as Efficient Oxygen Reduction Catalysts. ACS Applied Materials & Interfaces, 2017, 9, 9699-9709.	8.0	196
12	Atomic Feâ€Doped MOFâ€Derived Carbon Polyhedrons with High Activeâ€Center Density and Ultraâ€High Performance toward PEM Fuel Cells. Advanced Energy Materials, 2019, 9, 1802856.	19.5	196
13	High-performance Pd–Au bimetallic catalyst with mesoporous silica nanoparticles as support and its catalysis of cinnamaldehyde hydrogenation. Journal of Catalysis, 2012, 291, 36-43.	6.2	195
14	Novel Functionalized Nano-TiO ₂ Loading Electrocatalytic Membrane for Oily Wastewater Treatment. Environmental Science & Technology, 2012, 46, 6815-6821.	10.0	194
15	Review on the current practices and efforts towards pilot-scale production of metal-organic frameworks (MOFs). Coordination Chemistry Reviews, 2017, 352, 187-219.	18.8	190
16	Preparation and characterization of ZnO/TiO2, SO42â^'/ZnO/TiO2 photocatalyst and their photocatalysis. Journal of Photochemistry and Photobiology A: Chemistry, 2004, 168, 7-13.	3.9	167
17	Preparation of nitrogen-doped carbon nanotube arrays and their catalysis towards cathodic oxygen reduction in acidic and alkaline media. Carbon, 2012, 50, 2620-2627.	10.3	167
18	Single-Atom Catalysts for Electrochemical Hydrogen Evolution Reaction: Recent Advances and Future Perspectives. Nano-Micro Letters, 2020, 12, 21.	27.0	159

#	Article	IF	CITATIONS
19	High performance Pd-based catalysts for oxidation of formic acid. Journal of Power Sources, 2008, 180, 205-208.	7.8	154
20	g-C ₃ N ₄ promoted MOF derived hollow carbon nanopolyhedra doped with high density/fraction of single Fe atoms as an ultra-high performance non-precious catalyst towards acidic ORR and PEM fuel cells. Journal of Materials Chemistry A, 2019, 7, 5020-5030.	10.3	152
21	Formation of a Tubular Assembly by Ultrathin Ti _{0.8} Co _{0.2} N Nanosheets as Efficient Oxygen Reduction Electrocatalysts for Hydrogen–/Metal–Air Fuel Cells. ACS Catalysis, 2018, 8, 8970-8975.	11.2	147
22	Efficient hydrogen peroxide synthesis by metal-free polyterthiophene <i>via</i> photoelectrocatalytic dioxygen reduction. Energy and Environmental Science, 2020, 13, 238-245.	30.8	146
23	Tuning the Catalytic Activity of Ru@Pt Core–Shell Nanoparticles for the Oxygen Reduction Reaction by Varying the Shell Thickness. Journal of Physical Chemistry C, 2013, 117, 1748-1753.	3.1	140
24	Limitations and Improvement Strategies for Early-Transition-Metal Nitrides as Competitive Catalysts toward the Oxygen Reduction Reaction. ACS Catalysis, 2016, 6, 6165-6174.	11.2	130
25	Binary Fe, Cu-doped bamboo-like carbon nanotubes as efficient catalyst for the oxygen reduction reaction. Nano Energy, 2017, 37, 187-194.	16.0	125
26	Phosphorus and Nitrogen Dual Doped and Simultaneously Reduced Graphene Oxide with High Surface Area as Efficient Metal-Free Electrocatalyst for Oxygen Reduction. Catalysts, 2015, 5, 981-991.	3.5	122
27	Metal-organic framework as a host for synthesis of nanoscale Co3O4 as an active catalyst for CO oxidation. Catalysis Communications, 2011, 12, 875-879.	3.3	120
28	An Isolated Zinc–Cobalt Atomic Pair for Highly Active and Durable Oxygen Reduction. Angewandte Chemie, 2019, 131, 2648-2652.	2.0	116
29	Binary transition metal nitrides with enhanced activity and durability for the oxygen reduction reaction. Journal of Materials Chemistry A, 2015, 3, 16801-16809.	10.3	115
30	Photo- and thermally induced coloration of a crystalline MOF accompanying electron transfer and long-lived charge separation in a stable host–guest system. Chemical Communications, 2012, 48, 8114.	4.1	112
31	Advanced Atomically Dispersed Metal–Nitrogen–Carbon Catalysts Toward Cathodic Oxygen Reduction in PEM Fuel Cells. Advanced Energy Materials, 2021, 11, 2101222.	19.5	109
32	Uniform nitrogen and sulfur co-doped carbon nanospheres as catalysts for the oxygen reduction reaction. Carbon, 2014, 69, 294-301.	10.3	106
33	Nitrogen-doped graphene prepared by a transfer doping approach forÂthe oxygen reduction reaction application. Journal of Power Sources, 2014, 245, 801-807.	7.8	102
34	Cobalt and Nitrogen Codoped Graphene with Inserted Carbon Nanospheres as an Efficient Bifunctional Electrocatalyst for Oxygen Reduction and Evolution. ACS Sustainable Chemistry and Engineering, 2016, 4, 4131-4136.	6.7	101
35	Two-Dimensional Bimetallic Zn/Fe-Metal-Organic Framework (MOF)-Derived Porous Carbon Nanosheets with a High Density of Single/Paired Fe Atoms as High-Performance Oxygen Reduction Catalysts. ACS Applied Materials & Interfaces, 2020, 12, 13878-13887.	8.0	100
36	A high-performance composite ORR catalyst based on the synergy between binary transition metal nitride and nitrogen-doped reduced graphene oxide. Journal of Materials Chemistry A, 2017, 5, 5829-5837.	10.3	93

#	Article	IF	CITATIONS
37	In situ growth of cobalt sulfide hollow nanospheres embedded in nitrogen and sulfur co-doped graphene nanoholes as a highly active electrocatalyst for oxygen reduction and evolution. Journal of Materials Chemistry A, 2017, 5, 12354-12360.	10.3	93
38	Fluorescent and photochromic bifunctional molecular switch based on a stable crystalline metal-viologen complex. Chemical Communications, 2012, 48, 11641.	4.1	84
39	High-Performance Core–Shell Catalyst with Nitride Nanoparticles as a Core: Well-Defined Titanium Copper Nitride Coated with an Atomic Pt Layer for the Oxygen Reduction Reaction. ACS Catalysis, 2017, 7, 3810-3817.	11.2	84
40	High-Performance Doped Carbon Catalyst Derived from Nori Biomass with Melamine Promoter. Electrochimica Acta, 2014, 138, 353-359.	5.2	83
41	Photoassisted Oxygen Reduction Reaction in H ₂ –O ₂ Fuel Cells. Angewandte Chemie - International Edition, 2016, 55, 14748-14751.	13.8	81
42	Assessing the Influence of Side-Chain and Main-Chain Aromatic Benzyltrimethyl Ammonium on Anion Exchange Membranes. ACS Applied Materials & Interfaces, 2014, 6, 7585-7595.	8.0	79
43	Pt nanoparticles entrapped in titanate nanotubes (TNT) for phenol hydrogenation: the confinement effect of TNT. Chemical Communications, 2014, 50, 2794.	4.1	76
44	Coupling hollow Fe3O4 nanoparticles with oxygen vacancy on mesoporous carbon as a high-efficiency ORR electrocatalyst for Zn-air battery. Journal of Colloid and Interface Science, 2020, 567, 410-418.	9.4	75
45	Correlation between the photoactive character and the structures of two novel metal organic frameworks. Journal of Materials Chemistry, 2011, 21, 7895.	6.7	73
46	UIOâ€66â€NH ₂ â€Derived Mesoporous Carbon Catalyst Coâ€Doped with Fe/N/S as Highly Efficient Cathode Catalyst for PEMFCs. Small, 2019, 15, e1803520.	10.0	73
47	Core–Shell-Structured Low-Platinum Electrocatalysts for Fuel Cell Applications. Electrochemical Energy Reviews, 2018, 1, 324-387.	25.5	72
48	Hollow Loofahâ€Like N, Oâ€Coâ€Doped Carbon Tube for Electrocatalysis of Oxygen Reduction. Advanced Functional Materials, 2019, 29, 1900015.	14.9	68
49	Effects of Pt/C, Pd/C and PdPt/C anode catalysts on the performance and stability of air breathing direct formic acid fuel cells. International Journal of Hydrogen Energy, 2011, 36, 8518-8524.	7.1	67
50	Pd nanoparticles decorating flower-like Co ₃ O ₄ nanowire clusters to form an efficient, carbon/binder-free cathode for Li–O ₂ batteries. Journal of Materials Chemistry A, 2015, 3, 15626-15632.	10.3	67
51	Simultaneous doping of nitrogen and fluorine into reduced graphene oxide: A highly active metal-free electrocatalyst for oxygen reduction. Carbon, 2016, 99, 272-279.	10.3	65
52	Improving Potassium-Ion Batteries by Optimizing the Composition of Prussian Blue Cathode. ACS Applied Energy Materials, 2019, 2, 6528-6535.	5.1	65
53	High-Performance, Ultralow Platinum Membrane Electrode Assembly Fabricated by In Situ Deposition of a Pt Shell Layer on Carbon-Supported Pd Nanoparticles in the Catalyst Layer Using a Facile Pulse Electrodeposition Approach. ACS Catalysis, 2015, 5, 4318-4324.	11.2	64
54	A hybrid metal phosphate–phosphite material grafted with electron deficient organic components showing interesting fluorescent and photosensitive properties. Journal of Materials Chemistry A, 2013, 1, 4945.	10.3	63

#	Article	IF	CITATIONS
55	Hydrogen storage in Zr-fumarate MOF. International Journal of Hydrogen Energy, 2015, 40, 10542-10546.	7.1	63
56	Alkali resistant cross-linked poly(arylene ether sulfone)s membranes containing aromatic side-chain quaternary ammonium groups. Journal of Membrane Science, 2015, 474, 187-195.	8.2	63
57	From <i>Chlorella</i> to Nestlike Framework Constructed with Doped Carbon Nanotubes: A Biomass-Derived, High-Performance, Bifunctional Oxygen Reduction/Evolution Catalyst. ACS Applied Materials & Interfaces, 2017, 9, 32168-32178.	8.0	63
58	Anodic oxidation of ethanol on core-shell structured Ru@PtPd/C catalyst in alkaline media. Journal of Power Sources, 2011, 196, 6138-6143.	7.8	62
59	Antiperovskite Nitrides CuNCo _{3–<i>x</i>} V _{<i>x</i>} : Highly Efficient and Durable Electrocatalysts for the Oxygen-Evolution Reaction. Nano Letters, 2019, 19, 7457-7463.	9.1	62
60	MOF-Templated sword-like Co3O4@NiCo2O4 sheet arrays on carbon cloth as highly efficient Li–O2 battery cathode. Journal of Power Sources, 2020, 450, 227725.	7.8	62
61	Ruthenium nanoparticles mounted on multielement co-doped graphene: an ultra-high-efficiency cathode catalyst for Li–O ₂ batteries. Journal of Materials Chemistry A, 2015, 3, 11224-11231.	10.3	61
62	Hierarchically open-porous carbon networks enriched with exclusive Fe–Nx active sites as efficient oxygen reduction catalysts towards acidic H2–O2 PEM fuel cell and alkaline Zn–air battery. Chemical Engineering Journal, 2020, 390, 124479.	12.7	61
63	Preparation of anatase F doped TiO2 sol and its performance for photodegradation of formaldehyde. Journal of Materials Science, 2007, 42, 8193-8202.	3.7	58
64	Design of ultralong-life Li–CO ₂ batteries with IrO ₂ nanoparticles highly dispersed on nitrogen-doped carbon nanotubes. Journal of Materials Chemistry A, 2020, 8, 3763-3770.	10.3	58
65	Mesoporous carbon confined intermetallic nanoparticles as highly durable electrocatalysts for the oxygen reduction reaction. Journal of Materials Chemistry A, 2020, 8, 15822-15828.	10.3	58
66	High-performance PdRu bimetallic catalyst supported on mesoporous silica nanoparticles for phenol hydrogenation. Applied Surface Science, 2014, 315, 138-143.	6.1	56
67	Highly stable photochromic crystalline material based on a close-packed layered metal–viologen coordination polymer. Journal of Materials Chemistry, 2012, 22, 17452.	6.7	55
68	Nitrogen, phosphorus and iron doped carbon nanospheres with high surface area and hierarchical porous structure for oxygen reduction. Journal of Power Sources, 2015, 288, 253-260.	7.8	55
69	Enhanced Li-O2 battery performance, using graphene-like nori-derived carbon as the cathode and adding Lil in the electrolyte as a promoter. Electrochimica Acta, 2016, 200, 231-238.	5.2	55
70	Pd nano-particles (NPs) confined in titanate nanotubes (TNTs) for hydrogenation of cinnamaldehyde. Catalysis Communications, 2015, 59, 184-188.	3.3	54
71	Biomass-derived porous heteroatom-doped carbon spheres as a high-performance catalyst for the oxygen reduction reaction. International Journal of Hydrogen Energy, 2016, 41, 14101-14110.	7.1	54
72	High-performance doped carbon electrocatalyst derived from soybean biomass and promoted by zinc chloride. International Journal of Hydrogen Energy, 2014, 39, 10128-10134.	7.1	53

#	Article	IF	CITATIONS
73	Conversion of polystyrene foam to a high-performance doped carbon catalyst with ultrahigh surface area and hierarchical porous structures for oxygen reduction. Journal of Materials Chemistry A, 2014, 2, 12240-12246.	10.3	52
74	Prussian Blue [K ₂ FeFe(CN) ₆] Doped with Nickel as a Superior Cathode: An Efficient Strategy To Enhance Potassium Storage Performance. ACS Sustainable Chemistry and Engineering, 2019, 7, 16659-16667.	6.7	52
75	A Co-doped porous niobium nitride nanogrid as an effective oxygen reduction catalyst. Journal of Materials Chemistry A, 2017, 5, 14278-14285.	10.3	51
76	Uniform nitrogen and sulphur co-doped hollow carbon nanospheres as efficient metal-free electrocatalysts for oxygen reduction. Journal of Materials Chemistry A, 2017, 5, 1742-1748.	10.3	51
77	Design and Fabrication of a Dualâ€Photoelectrode Fuel Cell towards Costâ€Effective Electricity Production from Biomass. ChemSusChem, 2017, 10, 99-105.	6.8	51
78	Synthesis and characterization of visible light responsive N–TiO2 mixed crystal by a modified hydrothermal process. Journal of Non-Crystalline Solids, 2008, 354, 3965-3972.	3.1	50
79	Self-humidification of a PEM fuel cell using a novel Pt/SiO2/C anode catalyst. International Journal of Hydrogen Energy, 2010, 35, 7874-7880.	7.1	50
80	An effective Pd-promoted gold catalyst supported on mesoporous silica particles for the oxidation of benzyl alcohol. Applied Catalysis B: Environmental, 2013, 140-141, 419-425.	20.2	50
81	Series-connected hexacations cross-linked anion exchange membranes for diffusion dialysis in acid recovery. Journal of Membrane Science, 2019, 570-571, 120-129.	8.2	50
82	Regenerative fuel cells: Recent progress, challenges, perspectives and their applications for space energy system. Applied Energy, 2021, 283, 116376.	10.1	50
83	Ordered hierarchical mesoporous anatase TiO2 from yeast biotemplates. Colloids and Surfaces B: Biointerfaces, 2009, 74, 274-278.	5.0	49
84	Ultra-high-performance doped carbon catalyst derived from o-phenylenediamine and the probable roles of Fe and melamine. Applied Catalysis B: Environmental, 2014, 158-159, 60-69.	20.2	49
85	Cross-linked multiblock copoly(arylene ether sulfone) ionomer/nano-ZrO ₂ composite anion exchange membranes for alkaline fuel cells. RSC Advances, 2014, 4, 41398-41410.	3.6	49
86	High-performance gold-promoted palladium catalyst towards the hydrogenation of phenol with mesoporous hollow spheres as support. Catalysis Communications, 2012, 17, 29-33.	3.3	48
87	Highly Selective TiN-Supported Highly Dispersed Pt Catalyst: Ultra Active toward Hydrogen Oxidation and Inactive toward Oxygen Reduction. ACS Applied Materials & amp; Interfaces, 2018, 10, 3530-3537.	8.0	48
88	Tuning hydrophobic-hydrophilic balance of cathode catalyst layer to improve cell performance of proton exchange membrane fuel cell (PEMFC) by mixing polytetrafluoroethylene (PTFE). Electrochimica Acta, 2018, 277, 110-115.	5.2	47
89	Template-Free Preparation of 3D Porous Co-Doped VN Nanosheet-Assembled Microflowers with Enhanced Oxygen Reduction Activity. ACS Applied Materials & Interfaces, 2018, 10, 11604-11612.	8.0	47
90	Molecular packing, crystal to crystal transformation, electron transfer behaviour, and photochromic and fluorescent properties of three hydrogen-bonded supramolecular complexes containing benzenecarboxylate donors and viologen acceptors. RSC Advances, 2014, 4, 42983-42990.	3.6	46

#	Article	IF	CITATIONS
91	Tin and Silicon Binary Oxide on the Carbon Support of a Pt Electrocatalyst with Enhanced Activity and Durability. ACS Catalysis, 2015, 5, 2242-2249.	11.2	46
92	IrO2 nanoparticles highly dispersed on nitrogen-doped carbon nanotubes as an efficient cathode catalyst for high-performance Li-O2 batteries. Ceramics International, 2017, 43, 14082-14089.	4.8	46
93	Enhanced water management in the cathode of an air-breathing PEMFC using a dual catalyst layer and optimizing the gas diffusion and microporous layers. International Journal of Hydrogen Energy, 2015, 40, 3961-3967.	7.1	45
94	In situ construction of Ir@Pt/C nanoparticles in the cathode layer of membrane electrode assemblies with ultra-low Pt loading and high Pt exposure. Journal of Power Sources, 2017, 355, 83-89.	7.8	45
95	Recent advances in nanostructured transition metal nitrides for fuel cells. Journal of Materials Chemistry A, 2020, 8, 20803-20818.	10.3	45
96	Enhanced cyclability of Li–O ₂ batteries with cathodes of Ir and MnO ₂ supported on well-defined TiN arrays. Nanoscale, 2018, 10, 2983-2989.	5.6	44
97	Heteroatom-doped carbon nanorods with improved electrocatalytic activity toward oxygen reduction in an acidic medium. Carbon, 2014, 69, 132-141.	10.3	43
98	Enhancing the cyclability of Li–O 2 batteries using PdM alloy nanoparticles anchored on nitrogen-doped reduced graphene as the cathode catalyst. Journal of Power Sources, 2017, 337, 173-179.	7.8	43
99	Copper based metal–organic molecular ring with inserted Keggin-type polyoxometalate: a stable photofunctional host–guest molecular system. Chemical Communications, 2012, 48, 6154.	4.1	42
100	Design, fabrication and performance evaluation of a miniature air breathing direct formic acid fuel cell based on printed circuit board technology. Journal of Power Sources, 2010, 195, 7332-7337.	7.8	41
101	Preparation and characterization of core–shell structured catalysts using PtxPdy as active shell and nano-sized Ru as core for potential direct formic acid fuel cell application. Electrochimica Acta, 2011, 56, 2024-2030.	5.2	41
102	A core–shell Pd ₁ Ru ₁ Ni ₂ @Pt/C catalyst with a ternary alloy core and Pt monolayer: enhanced activity and stability towards the oxygen reduction reaction by the addition of Ni. Journal of Materials Chemistry A, 2016, 4, 847-855.	10.3	40
103	A mesoporous hollow silica sphere (MHSS): Synthesis through a facile emulsion approach and application of support for high performance Pd/MHSS catalyst for phenol hydrogenation. Applied Surface Science, 2011, 257, 4472-4477.	6.1	39
104	Oxygen reduction reaction operated on magnetically-modified PtFe/C electrocatalyst. International Journal of Hydrogen Energy, 2010, 35, 942-948.	7.1	38
105	Synthesis of a 3D photochromic coordination polymer with an interpenetrating arrangement: crystal engineering for electron transfer between donor and acceptor units. CrystEngComm, 2012, 14, 5137.	2.6	38
106	A renewable wood-derived cathode for Li–O ₂ batteries. Journal of Materials Chemistry A, 2018, 6, 14291-14298.	10.3	38
107	A strategy to unlock the potential of CrN as a highly active oxygen reduction reaction catalyst. Journal of Materials Chemistry A, 2020, 8, 8575-8585.	10.3	38
108	Synthesis and structure of a mixed crystal containing tris(4-pyridiniumyl)-1,3,5-triazine and benzenetetracarboxylate ions: constructing a new photochromic molecular system viaself-assembly. CrystEngComm, 2012, 14, 786-788.	2.6	37

#	Article	IF	CITATIONS
109	Hybrid PdAg alloy-Au nanorods: Controlled growth, optical properties and electrochemical catalysis. Nano Research, 2013, 6, 571-580.	10.4	37
110	Vesicular nitrogen doped carbon material derived from Fe2O3 templated polyaniline as improved non-platinum fuel cell cathode catalyst. Electrochimica Acta, 2013, 99, 30-37.	5.2	37
111	A hollow spherical doped carbon catalyst derived from zeolitic imidazolate framework nanocrystals impregnated/covered with iron phthalocyanines. Journal of Materials Chemistry A, 2016, 4, 7859-7868.	10.3	37
112	Versatile Route To Fabricate Precious-Metal Phosphide Electrocatalyst for Acid-Stable Hydrogen Oxidation and Evolution Reactions. ACS Applied Materials & Interfaces, 2020, 12, 11737-11744.	8.0	37
113	Nitrogen, Sulfur Co-doped Carbon Derived from Naphthalene-Based Covalent Organic Framework as an Efficient Catalyst for Oxygen Reduction. ACS Applied Energy Materials, 2018, 1, 161-166.	5.1	36
114	Emerging applications of atomic layer deposition for lithium-sulfur and sodium-sulfur batteries. Energy Storage Materials, 2020, 26, 513-533.	18.0	36
115	Nodal PtNi nanowires with Pt skin and controllable Near-Surface composition for enhanced oxygen reduction electrocatalysis in fuel cells. Chemical Engineering Journal, 2021, 418, 129322.	12.7	36
116	Platinum free ternary electrocatalysts prepared via organic colloidal method for oxygen reduction. Electrochemistry Communications, 2008, 10, 523-526.	4.7	35
117	High performance LiFePO4 microsphere composed of nanofibers with an alcohol-thermal approach. Journal of Materials Chemistry A, 2013, 1, 4546.	10.3	35
118	Effects of Metal lons and Ligand Functionalization on Hydrogen Storage in Metal–Organic Frameworks by Spillover. Journal of Physical Chemistry C, 2011, 115, 13829-13836.	3.1	34
119	Selenium-Functionalized Carbon as a Support for Platinum Nanoparticles with Improved Electrochemical Properties for the Oxygen Reduction Reaction and CO Tolerance. Journal of the Electrochemical Society, 2013, 160, H266-H270.	2.9	34
120	Nitrogen and Fluorine co-doped carbon catalyst with high oxygen reduction performance, prepared by pyrolyzing a mixture of melamine and PTFE. Electrochimica Acta, 2015, 182, 963-970.	5.2	34
121	Fog-like fluffy structured N-doped carbon with a superior oxygen reduction reaction performance to a commercial Pt/C catalyst. Nanoscale, 2015, 7, 3780-3785.	5.6	34
122	Enhanced low-humidity performance in a proton exchange membrane fuel cell by developing a novel hydrophilic gas diffusion layer. International Journal of Hydrogen Energy, 2020, 45, 937-944.	7.1	34
123	Dendrite-Free Composite Li Anode Assisted by Ag Nanoparticles in a Wood-Derived Carbon Frame. ACS Applied Materials & Interfaces, 2019, 11, 18361-18367.	8.0	33
124	A biocompatible drug delivery nanovalve system on the surface of mesoporous nanoparticles. Microporous and Mesoporous Materials, 2012, 147, 200-204.	4.4	32
125	High porosity and surface area self-doped carbon derived from polyacrylonitrile as efficient electrocatalyst towards oxygen reduction. Journal of Power Sources, 2016, 324, 134-141.	7.8	31
126	Effect of confinement of TiO 2 nanotubes over the Ru nanoparticles on Fischer-Tropsch synthesis. Applied Catalysis A: General, 2016, 526, 45-52.	4.3	31

#	Article	IF	CITATIONS
127	Integration of single Co atoms and Ru nanoclusters boosts the cathodic performance of nitrogen-doped 3D graphene in lithium–oxygen batteries. Journal of Materials Chemistry A, 2021, 9, 10747-10757.	10.3	31
128	Optimizing the Electronic Structure of Ordered Pt–Co–Ti Ternary Intermetallic Catalyst to Boost Acidic Oxygen Reduction. ACS Catalysis, 2022, 12, 7571-7578.	11.2	31
129	Pulse electrodeposition to prepare core–shell structured AuPt@Pd/C catalyst for formic acid fuel cell application. Journal of Power Sources, 2014, 246, 659-666.	7.8	30
130	Facile one-pot approach to the synthesis of spherical mesoporous silica nanoflowers with hierarchical pore structure. Applied Surface Science, 2014, 314, 7-14.	6.1	30
131	Three-Dimensional Biocarbon Framework Coupled with Uniformly Distributed FeSe Nanoparticles Derived from Pollen as Bifunctional Electrocatalysts for Oxygen Electrode Reactions. ACS Applied Materials & Interfaces, 2018, 10, 32133-32141.	8.0	29
132	Enhancing membrane electrode assembly performance by improving the porous structure and hydrophobicity of the cathode catalyst layer. Journal of Power Sources, 2019, 443, 227284.	7.8	29
133	Highly conductive and permselective anion exchange membranes for electrodialysis desalination with series-connected dications appending flexible hydrophobic tails. Desalination, 2020, 474, 114184.	8.2	29
134	Self-humidifying membrane electrode assembly prepared by adding PVA as hygroscopic agent in anode catalyst layer. International Journal of Hydrogen Energy, 2012, 37, 12860-12867.	7.1	28
135	Two-step oxalate approach for the preparation of high performance LiNi0.5Mn1.5O4 cathode material with high voltage. Journal of Power Sources, 2014, 247, 437-443.	7.8	28
136	On the limiting Stokes wave of extreme height in arbitrary water depth. Journal of Fluid Mechanics, 2018, 843, 653-679.	3.4	28
137	Rationally Designed Three-Dimensional N-Doped Graphene Architecture Mounted with Ru Nanoclusters as a High-Performance Air Cathode for Lithium–Oxygen Batteries. ACS Sustainable Chemistry and Engineering, 2020, 8, 6109-6117.	6.7	28
138	Synthesis of Core-shell Structured Ru@Pd/C Catalysts for the Electrooxidation of Formic Acid. Electrochimica Acta, 2017, 238, 194-201.	5.2	27
139	Nitrogen and atomic Fe dual-doped porous carbon nanocubes as superior electrocatalysts for acidic H2-O2 PEMFC and alkaline Zn-air battery. Journal of Energy Chemistry, 2021, 59, 388-395.	12.9	27
140	High-performance self-humidifying membrane electrode assembly prepared byÂsimultaneously adding inorganic and organic hygroscopic materials to the anode catalyst layer. Journal of Power Sources, 2013, 241, 367-372.	7.8	26
141	Enhanced performance of proton exchange membrane fuel cell by introducing nitrogen-doped CNTs in both catalyst layer and gas diffusion layer. Electrochimica Acta, 2017, 253, 142-150.	5.2	26
142	DFT study of high performance Pt3Sn alloy catalyst in oxygen reduction reaction. Computational Materials Science, 2018, 149, 107-114.	3.0	26
143	The Effect of PtRulr Nanoparticle Crystallinity in Electrocatalytic Methanol Oxidation. Materials, 2013, 6, 1621-1631.	2.9	25
144	Preparation and characterizations of platinum electrocatalysts supported on thermally treated CeO2–C composite support for polymer electrolyte membrane fuel cells. Electrochimica Acta, 2014, 139. 308-314.	5.2	25

#	Article	IF	CITATIONS
145	Photoassisted Oxygen Reduction Reaction in H ₂ –O ₂ Fuel Cells. Angewandte Chemie, 2016, 128, 14968-14971.	2.0	25
146	Alkylation of isobutane with butenes over solid acid catalysts. Applied Catalysis A: General, 1994, 107, 239-248.	4.3	24
147	A magnetic-field-assisted solution-phase route to cobalt thin film composed of cobalt nanosheets. Journal of Materials Chemistry, 2009, 19, 5207.	6.7	24
148	Platinum decorated Ru/C: Effects of decorated platinum on catalyst structure and performance for the methanol oxidation reaction. Journal of Power Sources, 2011, 196, 54-61.	7.8	24
149	A pulse electrochemical deposition method to prepare membrane electrode assemblies with ultra-low anode Pt loadings through in situ construction of active core–shell nanoparticles on an electrode. Journal of Power Sources, 2014, 260, 27-33.	7.8	24
150	Preparation and characterizations of highly dispersed carbon supported PdxPty/C catalysts by a modified citrate reduction method for formic acid electrooxidation. Journal of Power Sources, 2014, 254, 183-189.	7.8	24
151	Methanol tolerant core-shell RuFeSe@Pt/C catalyst for oxygen reduction reaction. International Journal of Hydrogen Energy, 2017, 42, 20658-20668.	7.1	24
152	Cobalt and Nitrogen Co-Doped Graphene-Carbon Nanotube Aerogel as an Efficient Bifunctional Electrocatalyst for Oxygen Reduction and Evolution Reactions. Catalysts, 2018, 8, 275.	3.5	24
153	Effect of the structure of Ni nanoparticles on the electrocatalytic activity of Ni@Pd/C for formic acid oxidation. International Journal of Hydrogen Energy, 2013, 38, 13125-13131.	7.1	23
154	Pt/graphene with intercalated carbon nanotube spacers introduced by electrostatic self-assembly for fuel cells. Materials Chemistry and Physics, 2019, 225, 371-378.	4.0	23
155	Biomass-derived 3D hierarchical N-doped porous carbon anchoring cobalt-iron phosphide nanodots as bifunctional electrocatalysts for Li O2 batteries. Journal of Power Sources, 2019, 412, 433-441.	7.8	23
156	Influence of hydrophobic components tuning of poly (aryl ether sulfone)s ionomers based anion exchange membranes on diffusion dialysis for acid recovery. Journal of Membrane Science, 2021, 636, 119562.	8.2	23
157	From Interwoven to Noninterpenetration: Crystal Structural Motifs of Two New Manganese–Organic Frameworks Mediated by the Substituted Group of the Bridging Ligand. European Journal of Inorganic Chemistry, 2008, 2008, 628-634.	2.0	22
158	Tuning the morphology of mesoporous silica by using various template combinations. Applied Surface Science, 2009, 255, 9365-9370.	6.1	22
159	Anion exchange membranes by bromination of benzylmethyl-containing poly(arylene ether)s for alkaline membrane fuel cells. RSC Advances, 2014, 4, 29682-29693.	3.6	22
160	A one-pot method to synthesize high performance multielement co-doped reduced graphene oxide catalysts for oxygen reduction. Electrochemistry Communications, 2014, 47, 49-53.	4.7	22
161	Enhanced low-humidity performance in a proton exchange membrane fuel cell by the insertion of microcrystalline cellulose between the gas diffusion layer and the anode catalyst layer. International Journal of Hydrogen Energy, 2015, 40, 15613-15621.	7.1	22
162	Platinum nanoparticles on carbon-nanotube support prepared by room-temperature reduction with H2 in ethylene glycol/water mixed solvent as catalysts for polymer electrolyte membrane fuel cells. Journal of Power Sources, 2016, 306, 448-453.	7.8	22

#	Article	IF	CITATIONS
163	Influence of the ions distribution of anion-exchange membranes on electrodialysis. Desalination, 2018, 437, 34-44.	8.2	22
164	Observation of two coupled Faraday waves in a vertically vibrating Hele-Shaw cell with one of them oscillating horizontally. Physics of Fluids, 2018, 30, 012108.	4.0	22
165	A 4-cell miniature direct formic acid fuel cell stack with independent fuel reservoir: Design and performance investigation. Journal of Power Sources, 2011, 196, 5913-5917.	7.8	21
166	Electrostatic interaction based hollow Pt and Ru assemblies toward methanol oxidation. RSC Advances, 2012, 2, 7479.	3.6	21
167	Electrochemical Behavior of Spherical LiFePO4/C Nanomaterial in Aqueous Electrolyte, and Novel Aqueous Rechargeable Lithium Battery with LiFePO4/C anode. Electrochimica Acta, 2015, 177, 277-282.	5.2	21
168	Ultra-high-performance core–shell structured Ru@Pt/C catalyst prepared by a facile pulse electrochemical deposition method. Scientific Reports, 2015, 5, 11604.	3.3	21
169	Nitrogen self-doped carbon nanoparticles derived from spiral seaweeds for oxygen reduction reaction. RSC Advances, 2016, 6, 27535-27541.	3.6	21
170	Synthesis of flower-like Co microcrystals composed of Co nanoplates in water/ethanol mixed solvent. Journal Physics D: Applied Physics, 2008, 41, 065004.	2.8	20
171	Ptâ^§Ru/C catalysts synthesized by a two-stage polyol reduction process for methanol oxidation reaction. Journal of Power Sources, 2011, 196, 10570-10575.	7.8	20
172	High-performance membrane electrode assembly with multi-functional Pt/SnO2–SiO2/C catalyst for proton exchange membrane fuel cell operated under low-humidity conditions. International Journal of Hydrogen Energy, 2016, 41, 9197-9203.	7.1	20
173	Doped reduced graphene oxide mounted with IrO2 nanoparticles shows significantly enhanced performance as a cathode catalyst for Li-O2 batteries. Electrochimica Acta, 2016, 192, 431-438.	5.2	20
174	Rechargeable Zinc–Air Battery with Ultrahigh Power Density Based on Uniform N, Co Codoped Carbon Nanospheres. ACS Applied Materials & Interfaces, 2019, 11, 44153-44160.	8.0	20
175	Synthesis of Co submicrospheres self-assembled by Co nanosheets via a complexant-assisted hydrothermal approach. Journal of Magnetism and Magnetic Materials, 2010, 322, 30-35.	2.3	19
176	Enhancement of capacity at high charge/discharge rate and cyclic stability of LiFePO4/C by nickel doping. lonics, 2013, 19, 445-450.	2.4	19
177	Atomic platinum layer coated titanium copper nitride supported on carbon nanotubes for the methanol oxidation reaction. Electrochimica Acta, 2017, 248, 349-355.	5.2	19
178	Influence of 2,2′,6,6′â€ŧetramethyl biphenolâ€based anionâ€exchange membranes on the diffusion dialysis hydrochloride acid. Journal of Applied Polymer Science, 2017, 134, 45333.	s of 2.6	19
179	Nanoconfined Nitrogenâ€Doped Carbonâ€Coated Hierarchical TiCoN Composites with Enhanced ORR Performance. ChemElectroChem, 2018, 5, 2041-2049.	3.4	19
180	Highly effective and stable doped carbon catalyst with three-dimensional porous structure and well-covered Fe3C nanoparticles prepared with C3N4 and tannic acid as template/precursors. Journal of Power Sources, 2019, 417, 117-124.	7.8	19

#	Article	IF	CITATIONS
181	Highly permselective tadpole-type ionic anion exchange membranes for electrodialysis desalination. Journal of Membrane Science, 2020, 600, 117861.	8.2	19
182	A fast and simple electrochemical impedance spectroscopy measurement technique and its application in portable, low-cost instrument for impedimetric biosensing. Journal of Electroanalytical Chemistry, 2011, 657, 158-163.	3.8	18
183	Highly performed non-humidification membrane electrode assembly prepared with binary RuO2–SiO2 oxide supported Pt catalysts as anode. International Journal of Hydrogen Energy, 2012, 37, 13103-13109.	7.1	18
184	Effect of Ni Core Structure on the Electrocatalytic Activity of Pt-Ni/C in Methanol Oxidation. Materials, 2013, 6, 2689-2700.	2.9	18
185	Highly stable and active Pt electrocatalysts on TiO 2 -Co 3 O 4 -C composite support for polymer exchange membrane fuel cells. Electrochimica Acta, 2015, 154, 266-272.	5.2	18
186	A bi-functional WO3-based anode enables both energy storage and conversion in an intermediate-temperature fuel cell. Energy Storage Materials, 2018, 12, 79-84.	18.0	18
187	Hexyl-modified series-connected bipyridine and DABCO di-cations functionalized anion exchange membranes for electrodialysis desalination. Separation and Purification Technology, 2021, 265, 118526.	7.9	18
188	Hydrogen storage of multiwalled carbon nanotubes coated with Pd-Ni nanoparticles under moderate conditions. Science Bulletin, 2006, 51, 2959-2963.	1.7	17
189	Synthesis and Optical Properties of Thiol Functionalized CdSe/ZnS (Core/Shell) Quantum Dots by Ligand Exchange. Journal of Nanomaterials, 2014, 2014, 1-14.	2.7	17
190	Aqueous phase synthesis and characterizations of Pt nanoparticles by a modified citrate reduction method assisted by inorganic salt stabilization for PEMFCs. Electrochimica Acta, 2014, 134, 187-192.	5.2	16
191	An ultra high performance multi-element doped mesoporous carbon catalyst derived from poly(4-vinylpyridine). Journal of Materials Chemistry A, 2015, 3, 23512-23519.	10.3	16
192	Three dimensional palladium nanoflowers with enhanced electrocatalytic activity towards the anodic oxidation of formic acid. Journal of Materials Chemistry A, 2015, 3, 973-977.	10.3	16
193	Uniformly dispersed carbon-supported bimetallic ruthenium–platinum electrocatalysts for the methanol oxidation reaction. Journal of Materials Science, 2017, 52, 3457-3466.	3.7	16
194	In-situ formation of N doped hollow graphene Nanospheres/CNTs architecture with encapsulated Fe3C@C nanoparticles as efficient bifunctional oxygen electrocatalysts. Journal of Alloys and Compounds, 2020, 828, 154238.	5.5	16
195	A new 3-D microporous Ln(III)–Cu(I) framework constructed by pyridine-3,5-dicarboxylate. Journal of Coordination Chemistry, 2009, 62, 2290-2298.	2.2	15
196	Preparation and characterization of carbon-supported PtOs electrocatalysts via polyol reduction method for methanol oxidation reaction. Journal of Power Sources, 2014, 268, 824-830.	7.8	15
197	Mesoporous silica nanoparticle supported PdIr bimetal catalyst for selective hydrogenation, and the significant promotional effect of Ir. Applied Surface Science, 2015, 357, 558-563.	6.1	15
198	Applications of M/N/C analogue catalysts in PEM fuel cells and metal-air/oxygen batteries: Status quo, challenges and perspectives. Progress in Natural Science: Materials International, 2020, 30, 807-814.	4.4	15

#	Article	IF	CITATIONS
199	Method of Evaluation of Electron Transfer Kinetics of a Surface-Confined Redox System by Means of Fourier Transformed Square Wave Voltammetry. Analytical Chemistry, 2008, 80, 5666-5670.	6.5	14
200	A novel cesium hydrogen sulfate–zeolite inorganic composite electrolyte membrane for polymer electrolyte membrane fuel cell application. Journal of Power Sources, 2009, 193, 483-487.	7.8	14
201	Enhanced electro-oxidation of formic acid by a PdPt bimetallic catalyst on a CeO2-modified carbon support. Science China Chemistry, 2012, 55, 391-397.	8.2	14
202	High performance of core–shell structured Ir@Pt/C catalyst prepared by a facile pulse electrochemical deposition. Electrochemistry Communications, 2014, 46, 115-119.	4.7	14
203	Formic acid as additive for the preparation of high-performance FePO4 materials by spray drying method. Ceramics International, 2017, 43, 16652-16658.	4.8	14
204	Organic colloid method to prepare ultrafine cobalt nanoparticles with the size of 2Ânm. Solid State Communications, 2008, 145, 118-121.	1.9	13
205	Multi-block copolymers with fluorene-containing hydrophilic segments densely functionalized by side-chain quaternary ammonium groups as anion exchange membranes. RSC Advances, 2016, 6, 41453-41464.	3.6	13
206	Faraday waves in a Hele-Shaw cell. Physics of Fluids, 2018, 30, .	4.0	13
207	Uniform Nitrogen and Sulfur Co-doped Carbon Bowls for the Electrocatalyzation of Oxygen Reduction. ACS Sustainable Chemistry and Engineering, 2019, 7, 7148-7154.	6.7	13
208	Robust InNCo _{3–<i>x</i>} Mn <i>_{<i>x</i>}</i> Nitride-Supported Pt Nanoparticles as High-Performance Bifunctional Electrocatalysts for Zn–Air Batteries. ACS Applied Energy Materials, 2020, 3, 5293-5300.	5.1	13
209	Theoretical study of proton transfer in triflic acid/water, imidazole and pyrazole clusters. Computational and Theoretical Chemistry, 2009, 897, 66-68.	1.5	12
210	Ultrasonic-assisted ac etching of aluminum foils for electrolytic capacitor electrodes with enhanced capacitance. Materials Chemistry and Physics, 2010, 123, 625-628.	4.0	12
211	A layered zinc phosphate decorated with organic fluorophores for selective luminescent sensing of metal cations. Dalton Transactions, 2012, 41, 10910.	3.3	12
212	Binary oxide-doped Pt/RuO2–SiOx/C catalyst with high performance and self-humidification capability: The promotion of ruthenium oxide. Journal of Power Sources, 2012, 205, 201-206.	7.8	12
213	Platinum catalysts supported on Nafion functionalized carbon black for fuel cell application. Journal of Energy Chemistry, 2013, 22, 87-92.	12.9	12
214	Highly ordered and surfactant-free PtxRuy bimetallic nanocomposites synthesized by electrostatic self assembly for methanol oxidation reaction. Electrochimica Acta, 2013, 112, 431-438.	5.2	12
215	Highly active carbon supported palladium catalysts decorated by a trace amount of platinum by an in-situ galvanic displacement reaction for formic acid oxidation. Journal of Power Sources, 2015, 278, 332-339.	7.8	12
216	Improvement of proton exchange membrane fuel cell performance in low-humidity conditions by adding hygroscopic agarose powder to the catalyst layer. Journal of Power Sources, 2015, 273, 168-173.	7.8	12

#	Article	IF	CITATIONS
217	Platinum-decorated palladium-nanoflowers as high efficient low platinum catalyst towards oxygen reduction. International Journal of Hydrogen Energy, 2017, 42, 22909-22914.	7.1	12
218	High porosity nitrogen and phosphorous Co-doped carbon nanosheets as an efficient catalyst for oxygen reduction. International Journal of Hydrogen Energy, 2018, 43, 9749-9756.	7.1	12
219	Glucose-derived carbon supported well-dispersed CrN as competitive oxygen reduction catalysts in acidic medium. Electrochimica Acta, 2019, 314, 202-211.	5.2	12
220	A mesoporous carbon derived from 4,4′-dipyridyl iron as an efficient catalyst for oxygen reduction. Journal of Materials Chemistry A, 2020, 8, 2439-2444.	10.3	12
221	Steady-state multiple near resonances of periodic interfacial waves with rigid boundary. Physics of Fluids, 2020, 32, .	4.0	12
222	Immobilization of highly active Pd nano-catalysts on functionalized mesoporous silica supports using mercapto groups as anchoring sites and their catalytic performance for phenol hydrogenation. Chinese Journal of Catalysis, 2013, 34, 1519-1526.	14.0	11
223	High performance Pd catalyst using silica modified titanate nanotubes (STNT) as support and its catalysis toward hydrogenation of cinnamaldehyde at ambient temperature. RSC Advances, 2014, 4, 63062-63069.	3.6	11
224	Self-humidifying membrane electrode assembly prepared by adding microcrystalline cellulose in anode catalyst layer as preserve moisture. International Journal of Hydrogen Energy, 2014, 39, 12842-12848.	7.1	11
225	Synthesis of three-dimensional Pd nanospheres decorated with a Pt monolayer for the oxygen reduction reaction. International Journal of Hydrogen Energy, 2014, 39, 14018-14026.	7.1	11
226	Enhancement of Oxygen Reduction Performance of Biomass-Derived Carbon through Co-Doping with Early Transition Metal. Journal of the Electrochemical Society, 2018, 165, J3148-J3156.	2.9	11
227	In-situ IR monitoring to probe the formation of structural defects in Zr-fumarate metal–organic framework (MOF). Polyhedron, 2018, 153, 205-212.	2.2	11
228	Spinel LiMn ₂ O ₄ Nanoparticles Grown in Situ on Nitrogen-Doped Reduced Graphene Oxide as an Efficient Cathode for a Li-O ₂ /Li-Ion Twin Battery. ACS Sustainable Chemistry and Engineering, 2019, 7, 430-439.	6.7	11
229	Mono-disperse PdO nanoparticles prepared via microwave-assisted thermo-hydrolyzation with unexpectedly high activity for formic acid oxidation. Electrochimica Acta, 2020, 329, 135166.	5.2	11
230	Steady-state harmonic resonance of periodic interfacial waves with free-surface boundary conditions based on the homotopy analysis method. Journal of Fluid Mechanics, 2021, 916, .	3.4	10
231	UIO-66-NH ₂ -derived mesoporous carbon used as a high-performance anode for the potassium-ion battery. RSC Advances, 2021, 11, 1039-1049.	3.6	10
232	Effects of tailoring and dehydrated cross-linking on morphology evolution of ordered mesoporous carbons. RSC Advances, 2016, 6, 19515-19521.	3.6	9
233	MOF-Derived Carbon Materials Mounted with Highly Dispersed Ru and MoO ₃ for Rechargeable Li–O ₂ Cathode Yield Enhanced Cyclability. ACS Sustainable Chemistry and Engineering, 2019, 7, 2296-2303.	6.7	9
234	Methanol-tolerant Se^Pt/C: effects of Se content on the structure and electrocatalytic performance for oxygen reduction reaction. Ionics, 2020, 26, 1315-1323.	2.4	9

#	Article	IF	CITATIONS
235	Accurate predictions of chaotic motion of a free fall disk. Physics of Fluids, 2021, 33, .	4.0	9
236	Heterostructured Pd/Ti/Pd Thin Films as Highly Efficient Catalysts for Methanol and Formic Acid Oxidation. ACS Applied Materials & Interfaces, 2021, 13, 31725-31732.	8.0	9
237	Effects of Co doping sites on the electrochemical performance of LiNi0.5Mn1.5O4 as a cathode material. Ionics, 2020, 26, 3777-3783.	2.4	9
238	Theoretical study on sulfonated and phosphonated poly[(aryloxy)phosphazenes] as proton-conducting membranes for fuel cell applications. European Polymer Journal, 2009, 45, 2391-2394.	5.4	8
239	Volume production of high loading Pt/C catalyst with high performance via a microwave-assisted organic colloid route. Journal of Power Sources, 2012, 210, 54-59.	7.8	8
240	Synthesis and characterizations of palladium catalysts with high activity and stability for formic acid oxidation by hydrogen reduction in ethylene glycol at room temperature. Journal of Power Sources, 2015, 294, 556-561.	7.8	8
241	Construction of a high-performance air-breathing cathode using platinum catalyst supported by carbon black and carbon nanotubes. International Journal of Hydrogen Energy, 2016, 41, 9191-9196.	7.1	8
242	High oxygen reduction activity of TM13@Pt134 and TM12N@Pt134 (TM=Ti, V, Mn, Fe, Co, Ni, and Cu) core-shell electrocatalysts studied by first-principles theory. Materials Chemistry and Physics, 2018, 212, 378-384.	4.0	8
243	Highâ€Performance 3D Pineconeâ€Like LiNi 1/3 Co 1/3 Mn 1/3 O 2 Cathode for Lithiumâ€Ion Batteries. Energy Technology, 2019, 7, 1800769.	3.8	8
244	Yucca-like CoO–CoN Nanoarray with Abundant Oxygen Vacancies as a High-Performance Cathode for Lithium–Oxygen Batteries. ACS Applied Energy Materials, 2020, 3, 12000-12008.	5.1	8
245	Electrooxidation of methanol over a membrane-based electrode and effect of tungsten and molybdenum on the activity. Applied Catalysis A: General, 2002, 235, 149-155.	4.3	7
246	Bis(phenylammonium) tetrachloridozincate(II) monohydrate. Acta Crystallographica Section E: Structure Reports Online, 2007, 63, m2571-m2571.	0.2	7
247	A novel hollow sphere mesoporous material synthesized by using DADD template and embedding Nd into framework simultaneously. Microporous and Mesoporous Materials, 2008, 113, 261-267.	4.4	7
248	A Platinum Monolayer Core-Shell Catalyst with a Ternary Alloy Nanoparticle Core and Enhanced Stability for the Oxygen Reduction Reaction. Journal of Nanomaterials, 2015, 2015, 1-11.	2.7	7
249	Highly stable and efficient platinum nanoparticles supported on TiO 2 @Ru-C: investigations on the promoting effects of the interpenetrated TiO 2. Electrochimica Acta, 2016, 216, 8-15.	5.2	7
250	Platinum Nanoparticles on Interconnected Ni ₃ P/Carbon Nanotube–Carbon Nanofiber Hybrid Supports with Enhanced Catalytic Activity for Fuel Cells. ChemElectroChem, 2017, 4, 109-114.	3.4	7
251	Biogelatin-Derived and N,S-Codoped 3D Network Carbon Materials Anchored with RuO ₂ as an Efficient Cathode for Rechargeable Li–O ₂ Batteries. Journal of Physical Chemistry C, 2021, 125, 21914-21921.	3.1	7
252	Recent Development of Anode Electrocatalysts for Direct Methanol Fuel Cells. Chinese Journal of Catalysis, 2010, 31, 141-149.	14.0	7

#	Article	IF	CITATIONS
253	Anodic oxidation of ethanol on inorganic membrane-based electrodes. Applied Catalysis A: General, 2004, 258, 183-188.	4.3	6
254	Porous grape-like spherical silica with hydrogen storage capability, synthesized using neutral dual surfactants as templates. International Journal of Hydrogen Energy, 2009, 34, 3810-3815.	7.1	6
255	Preparation of large Co nanosheets with enhanced coercivity by a magnetic-field-assisted solvothermal approach free of surfactants, complexants or templates. Journal of Magnetism and Magnetic Materials, 2009, 321, 2566-2570.	2.3	6
256	High pressure organic colloid method for the preparation of high performance carbon nanotube-supported Pt and PtRu catalysts for fuel cell applications. Science China Technological Sciences, 2010, 53, 264-271.	4.0	6
257	Nitrogen-containing porous cerium trimetaphosphimate as a new efficient base catalyst. Journal of Materials Chemistry, 2011, 21, 6144.	6.7	6
258	Synthesis, characterization, and catalytic behavior of two open-framework zinc phosphites with 2D and 3D structures. Inorganic Chemistry Communication, 2011, 14, 150-154.	3.9	6
259	Effect of thermal treatment on structural change of anode electrocatalysts for direct methanol fuel cells. Particuology, 2014, 15, 45-50.	3.6	6
260	Organic-phase synthesis of Li3V2(PO4)3@Carbon nanocrystals and their lithium storage properties. RSC Advances, 2018, 8, 19335-19340.	3.6	6
261	Design of a Multispherical Cavity Carbon with In Situ Silica Modifications and Its Selfâ€Humidification Application on Fuel Cell Anode Support. Advanced Materials Interfaces, 2018, 5, 1800314.	3.7	6
262	In-situ grown vanadium nitride coated with thin layer of nitrogen-doped carbon as a highly durable binder-free cathode for Li–O2 batteries. Journal of Power Sources, 2020, 460, 228109.	7.8	6
263	LiFePO ₄ /C Microspheres with Nano-micro Structure, Prepared by Spray Drying Method Assisted with PVA as Template. Current Nanoscience, 2012, 8, 208-214.	1.2	5
264	Surfacial carbonized palygorskite as support for high-performance Pt-based electrocatalysts. Journal of Solid State Electrochemistry, 2013, 17, 2009-2015.	2.5	5
265	Enhanced durability and self-humidification of platinum catalyst through decoration with SnSi binary oxide. Journal of Applied Electrochemistry, 2018, 48, 1163-1173.	2.9	5
266	Enhanced low-humidity performance of proton-exchange membrane fuel cell by introducing hydrophilic CNTs in membrane electrode assembly. Progress in Natural Science: Materials International, 2022, 32, 150-156.	4.4	5
267	Synthesis and Properties of Symmetric Side hain Quaternized Poly(Arylene Ether Sulfone)s for Anion Exchange Membrane Fuel Cells. Macromolecular Chemistry and Physics, 2018, 219, 1700416.	2.2	4
268	Effect of Pt Oxidation State on Methanol Oxidation Activity. Chinese Journal of Catalysis, 2011, 32, 86-92.	14.0	3
269	An efficient basic catalyst based on a new germanium coordination complex. Inorganic Chemistry Communication, 2012, 15, 221-224.	3.9	3
270	Influence of Oxygen Contents on the Microstructure, High Temperature Oxidation and Corrosion Resistance Properties of Cr–Si–O–N Coatings. Coatings, 2018, 8, 19.	2.6	3

#	Article	IF	CITATIONS
271	MNi4.8Sn0.2(M=La, Nd)-supported multi-walled carbon nanotube composites as hydrogen storage materials. Science Bulletin, 2007, 52, 1616-1622.	1.7	2
272	Facile synthesis of high dispersion γ-Fe2O3–Au nanoparticles within mesoporous silica spheres. RSC Advances, 2015, 5, 49914-49919.	3.6	2
273	Enhanced performance of LiNi0.03Mo0.01Mn1.96O4 cathode materials coated with biomass-derived carbon layer. Ionics, 2019, 25, 917-925.	2.4	2
274	A comparative study on the catalytic activities and stabilities of atomic-layered platinum on dispersed Ti0.9Cu0.1N nanoparticles supported by N-doped carbon nanotubes (N-CNTs) and reduced graphene oxide (N-rGO). International Journal of Hydrogen Energy, 2020, 45, 1857-1866.	7.1	2
275	Metallic cobalt encapsulated in N-doped carbon nanowires: a highly active bifunctional catalyst for oxygen reduction and evolution. Ionics, 2021, 27, 3501-3509.	2.4	2
276	A Modified Solid-State Reduction Method to Prepare Supported Platinum Nanoparticle Catalysts for Low Temperature Fuel Cell Application. Current Nanoscience, 2009, 5, 252-256.	1.2	2
277	Effects of preparation conditions on the morphology and performance of palladium nanostructures. International Journal of Hydrogen Energy, 2019, 44, 1525-1533.	7.1	1
278	Methods for Remit Voltage Reversal of Proton Exchange Membrane Fuel Cells. Frontiers in Energy Research, 2022, 10, .	2.3	1
279	Diethylammonium ethyl (4-methylanilino)phosphonate chloroform solvate. Acta Crystallographica Section E: Structure Reports Online, 2007, 63, o3955-o3955.	0.2	0
280	Lithium-rich layered nickel–manganese oxides as high-performance cathode materials: the effects of composition and PEG on performance. Ionics, 2016, 22, 2067-2073.	2.4	0
281	Enforced Electrocatalytic Oxidation of Low Concentration of Phenol On the Porous Ceramic Tube Based Electrode Supported With Platinum Nanoparticles. Current Nanoscience, 2013, 9, 792-797.	1.2	Ο